EXPERIMENT AND SIMULATION OF A WIND-DRIVEN REVERSE OSMOSIS DESALINATION SYSTEM

Sang-Jin Park[1] and Clark C.K. Liu[2]

[1] Thermo-Fluid System Dept., Korea Institute of Machinery & Materials, Daejeon, Korea

[2] Dept. of Civil Engineering, University of Hawaii at Manoa, Honolulu, Hawaii, USA

Abstract: A mathematical model was developed to simulate the performance of a prototype wind-powered reverse osmosis desalination system. The model consists of two sub-models operated in a series. The first sub-model is the wind-energy conversion sub-model, which has wind energy and feed water as its input and pressurized feed water as its output. The second sub-model is a reverse osmosis (RO) process sub-model, with pressurized feed water as its input and the flow and salinity of the product water or permeate as its output. Model coefficients were determined based on field experiments of a prototype wind powered RO desalination system of the University of Hawaii, from June to December 2001. The mathematical model developed by this study predicts the performance of wind-powered RO desalination systems under different design conditions. The system optimization is achieved using a linear programming approach. Based on the results of system optimization, a design guide is prepared, which can be used by both manufacturer and end-user of the wind-driven reverse osmosis system.

Keywords: Desalination, Wind power, Reverse osmosis, Multi-blade windmill, Optimal design

1. INTRODUCTION

In the past, distillation like MSF (Multi-Stage Flash) or MED (Multi-Effect Distillation) was the most prevailing process in the field of saline water desalination and the portion of MSF and MED in the world's desalination capacity was about 70% in last decades. Lately, reverse osmosis process has been gaining popularity for purifying brackish water and seawater due to successive developments in membrane technology, so that the number of desalination units by reverse osmosis (RO) is more than any other methods now [Wangnick, 1996]. Reverse osmosis and nano-filtration (NF) are the most commonly used membrane processes for potable water treatment in the United States [AWWARF, et al., 1996]. In addition, within the last 10 years, RO has been applied to production of ultra-high-purity water for the pharmaceutical industry, the research laboratory, the hemo-dialysis process, and the manufacture of integrated circuits in the electronics industry [Parekh, 1988].

In general, a water treatment process is se-

lected on a cost and quality basis. Obviously, reverse osmosis is a well-established process in the production of potable water from brackish water and seawater. Up to now, however, application of RO process has been partly limited due to its highly energy intensive nature. In particular, the energy consumption per unit product gets much larger as system capacity decreases because energy saving devices like pressure recovery turbine are hardly applicable to a small scale unit. Thus, it may make small scale RO process inferior in competition with other alternatives. Consequently, many researches and developments have been focused on how to reduce the operating cost, especially in small capacity systems.

In many Pacific islands and coastal areas, the contamination of groundwater with seawater caused by over-pumping of groundwater and the increase of freshwater demand by remote small communities are bringing about interests in brackish water desalination. And reverse osmosis is regarded as one of the most attractive processes that can be applied to these situations. But the limited electric energy resource and its relatively high cost in these remote areas have stimulated researches for the development of cost-effective RO system using natural energies like ocean wave-powered RO [Hicks, et al., 1989], solar-powered RO [Abdul-Fattah, 1986] and wind-powered RO [Feron, 1985; Robinson, et al., 1992; Liu, et al., 2002]. Because wind power is more cost-effective than photovoltaic and hybrid wind - PV (photovoltaic) system for stand-alone power system [Kellogg, et al., 1998] and trade wind is one of the most feasible renewable natural energy in most islands and coastal areas, RO directly driven by a windmill has been frequently applied to this case. Low installation cost and easy purchase of a commercial multi-blade windmill are reasons why wind can be selected for power generator of a small RO system, regardless of its relatively lower energy efficiency (generally less than 0.3) Recently, innovations in membrane technology have promoted its realization, that is, the development of ultra-low pressure membrane makes it possible to purify brackish water under operating pressure of 600 – 1,500 kPa. Windpowered RO process becomes more practical.

Nevertheless, there are very few useful data for optimal design and operation of this process. For combination of wind-turbine electric generator and RO process, several useful researches have been reported about its feasibility, optimal design, and economic analysis [Voivontas, et al., 2001; Garcia-Rodriguez, et al., 2001; Houcine, et al., 1999; Kiranoudis, et al. 1997]. However, up to now, it is very rare to find a practical design guide for RO directly driven by a windmill. Consequently, it is difficult for manufacturers and end-users of this system to select and design appropriate system configuration, dimension, and operating condition for their own situations. These design variables are determined by average wind-speed, feed water concentration, and desired product rate. The objective of this work, which is a part of research efforts on wind-driven reverse osmosis desalination at the University of Hawaii at Manoa [Liu, et al., 2002], is to provide a design guide for a small capacity wind powered RO system. Optimal system design parameters are identified; the emphasis is to provide a simple, practical, and yet comprehensive relationship between input conditions and design variables.

2. PROTOTYPE SYSTEM

A reverse osmosis desalination system di-

rectly driven by a windmill consists of two processes; wind-energy conversion process and reverse osmosis separation process as shown in Fig. 1. In wind-energy conversion process, a pump coupled with a multi-blade windmill pressurizes feed water. And the RO process separates fresh water from feed water through a semi permeable membrane, where the dominant driving force is pressure difference across the membrane. In other words, the first process converts wind-energy into driving force for the second one. The system input is wind and raw water and the output is permeate (fresh water) and concentrate (brine).

The prototype desalination system of this work is located on Coconut Island, Oahu, Hawaii and consists of four major subsystems: windmill/pump, pressure stabilizer, reverse osmosis module, and control module. Figure 2 is a schematic diagram of the system. Feed water pumped by a piston pump directly driven by a windmill flows into a pressure stabilizer and then passes a cartridge filter to remove contaminants. And the filtrate is separated into permeate and concentrate in the RO module.

A typical multi-blade windmill is used and its diameter is 4.28 m (14 feet). The windmill is installed on a 9-meter tall tower and drives directly a piston pump whose stroke is 275 mm (11 inch) and effective displacement is 977 cm^3. Dempster Inc., USA, manufactured both the windmill and the pump.

In order to maintain the feed water pressure stable regardless of wind-speed fluctuation, a stabilizer was developed as a buffer. Actually, the high variability of wind and the pulsating discharge characteristic of the piston pump make flow rate and pressure of the feed very unstable and this may result in operation failure. The pressure stabilizer reduces excessive fluctuation of the pressure and the flow rate. The stabilizer in this work is a kind of hydro-pneumatic pressure tank and its inner volume is 0.3 m^3 that is corresponding to total feed volume of 30 minutes at design condition.

In general, pretreatment module prior to RO membrane is necessary to prevent fouling on the membrane surface due to contaminants in the feed. It is very important in seawater desalination and surface water purification so that a large amount of capital cost would be invested to it for stable membrane performance and elongation of the membrane lifetime. However, because it is well known that most well water contains very little contaminant like silt and microorganisms, just a cartridge filter with 5μm nominal removal rate was used as pretreatment process. The RO membrane element used in this work is a TFC-SC4040ULP of Fluid System Company. Its effective surface area is 7.43 m^2 (80 ft^2) and design pressure range is 345 – 1,210 kPa (50 – 175 psi). This element is one of typical ultra-low pressure membranes and it has been used for one year without C.I.P. (cleaning in process) or replacement.

The operating pressure of 517 – 724 kPa (75 – 105 psi) is maintained by a feedback control system. When the pressure in the stabilizer reaches at 517 kPa, the controller opens a solenoid valve to let the pressurized feed flow from stabilizer into cartridge filter and RO module. If the pressure is over 724 kPa, the relieve valve will be open to discharge the excess water from the stabilizer. In addition, concentrate flow control is employed in this system, which three parallel solenoid valves located at discharge port of the membrane module are opened/closed with respect to the pressure in the stabilizer. Introducing this control method, it is possible to operate the pilot stably and continuously in very

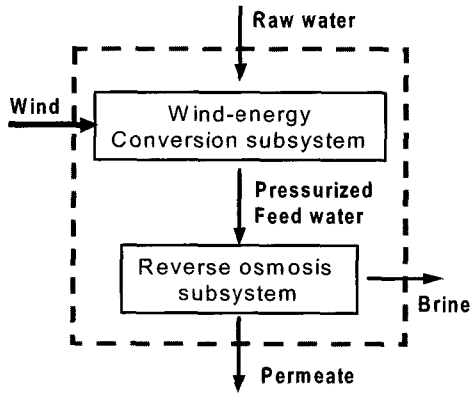

Fig.1 Wind-driven reverse osmosis desalination

mild or suddenly changing wind condition [Liu, et al., 2002].

3. MATHEMATICAL SIMULATION AND PREDICTION

Mathematical modeling has been carried out separately for each process in Fig. 1. First, empirical relationship between wind-energy and pumping performance was obtained from field test and then separation phenomena in RO process were formulated as a one-dimensional modeling. Model coefficients were determined based on the field experimental results. Finally, these two sub-models were integrated into a system simulation tool.

3.1 Sub-Model for Wind Energy Conversion Process

Available kinetic power of wind passing a windmill can be expressed as

$$P_{avail} = \frac{1}{2}\dot{m}_a U^2 = \frac{1}{2}\rho_a A U^3 \quad (1)$$

and power delivered to water by windmill/pump is

$$P_{deliv} = \rho_w g Q_w H \quad (2)$$

where $\dot{m}$ is mass flow rate, U is perpendicular component of the wind velocity to windmill rotating plane, A is area of windmill rotating plane, Q is flow rate, and H is hydraulic head [White, 1986]. The overall efficiency η is defined as ratio of delivered power to available power.

$$\eta \equiv \frac{P_{deliv}}{P_{avail}} = 2\frac{\rho_w g Q_w H}{\rho_a A U^3} \quad (3)$$

This includes efficiency of the pump and mechanical transmission efficiency as well as windmill efficiency.

3.2 Sub-Model for RO Process

The driving force of RO membrane process is pressure. Thus, water flow can be characterized as a function of pressure difference across the membrane. On the other hand, salt diffusion is generated by salinity gradient across the membrane. The basic diffusion transport equations used for water and salt flux are given as follows: [Merten, et al., 1964; Lonsdale, et al., 1965; Rosenfeld and Loeb, 1967]

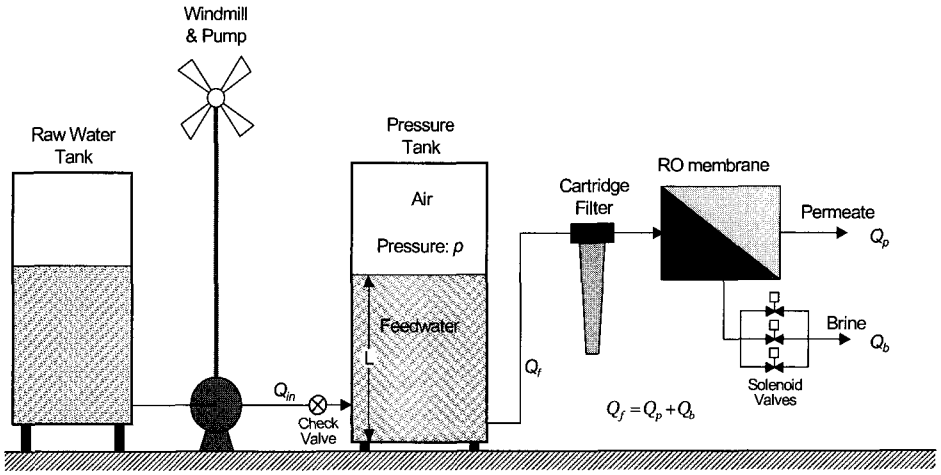

Fig. 2 Schematic diagram of the prototype system

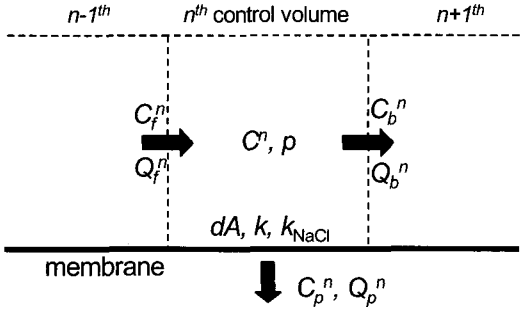

Fig. 3 Schematic diagram of the control volume for RO process modeling

water flux: $J = k_w(p - \Delta\pi)$ (4)

salt flux: $J_i \equiv C_p J = k_i(C - C_p)$ (5)

where k_w and k_i is permeability coefficient for pure-water and salt, respectively. And C is concentration and π is osmotic pressure. Osmotic pressure due to concentration difference may be calculated using Eq.(6) [Reynolds and Richards, 1996].

$$\Delta\pi(\text{kPa}) = 0.0779(C - C_p) \quad (6)$$

Combining Eq.(4) and Eq.(6), the water flux can be obtained as

$$J = k_w\{p - 0.0779(C - C_p)\} \quad (7)$$

In these equations, C is concentration on the membrane surface and it is higher than that of brine bulk flow because of concentration polarization in boundary layer [Denisov, 1994]. In addition to this, even concentration of brine bulk flow increases along the flow direction due to decrease of bulk flow rate. Hence, C is a function not only of feed concentration but also of brine flow rate, desalination ratio, Schmit number, Reynolds number and so forth [AWWARF, et al., 1996]. In this work, however, only longitudinal variation of brine concentration is taken

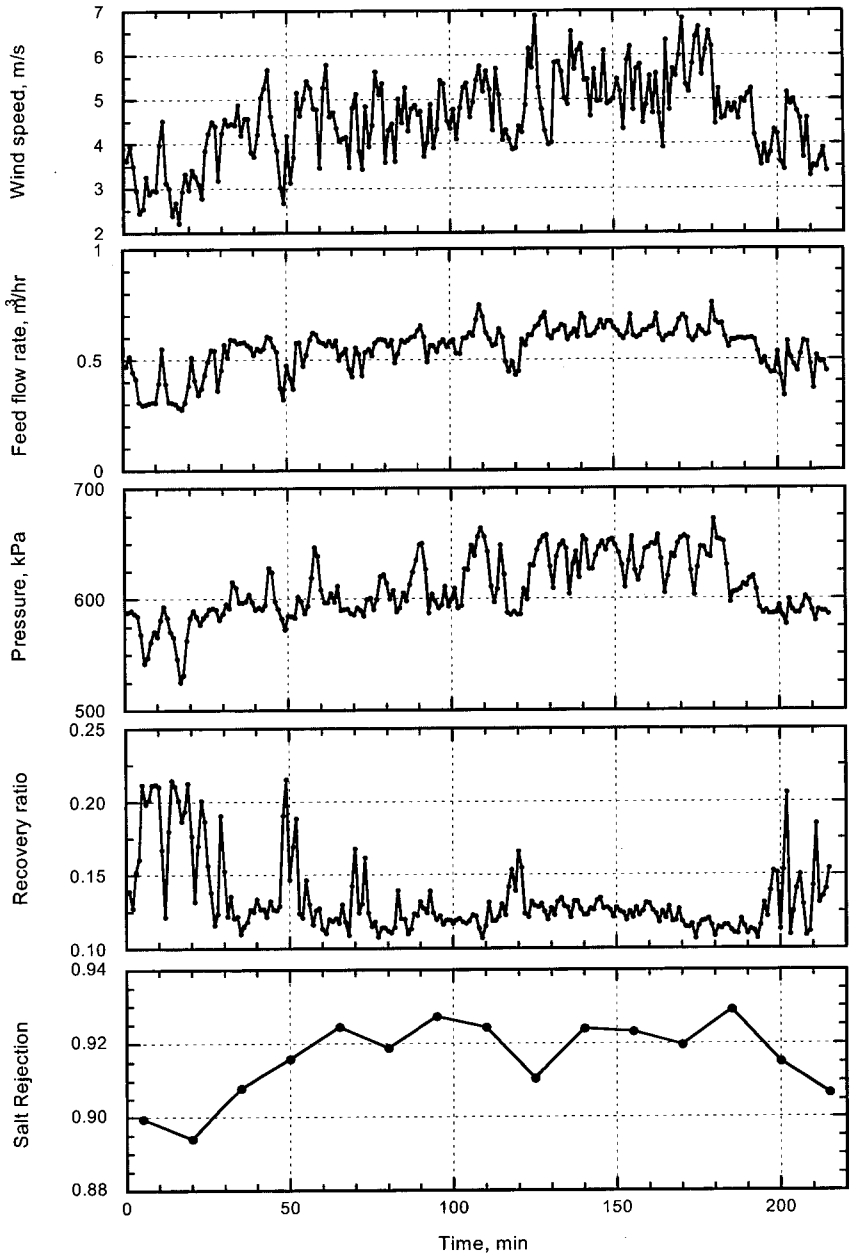

Fig. 4 Experimental result on August 24, 2001

into consideration for convenience of analysis. It may bring about an error but rough trend is hardly influenced by it. Therefore, concentration of brine bulk flow may be regarded as C. Consequently, one-dimensional modeling can be applied to RO membrane process.

For an infinitesimal control volume of a membrane element shown in Fig. 3, the varia-

tion of bulk concentration within the control volume is negligible. Permeate flow rate Q_p^n and concentration C_p^n may be obtained through some iterations for given Q_f^n, C_f^n, k_w, and k_i, where up-stream concentration C_f^n is used as C^n (up-wind scheme). From Eq. (5) and (7), Q_p^n and C_p^n for the control volume can be expressed as

$$Q_p^n = k_w \cdot dA \cdot \left\{p - 0.0779(C_f^n - C_p^n)\right\} \quad (8)$$

$$C_p^n = \frac{k_i \cdot dA \cdot C_f^n}{Q_p^n + k_i \cdot dA} \quad (9)$$

where dA is membrane area of a control volume. Operating pressure p is let to be a constant along the membrane surface because pressure drop over a membrane element is practically very small compared with inlet pressure ($\Delta p/p \leq 0.05$). These simultaneous equations in two unknowns can be solved by following steps: (a) guessing the initial value of C_p^n; (b) to calculate Q_p^n from Eq. (8); (c) to calculate C_p^n by substituting Q_p^n obtained in step b into Eq. (9); (d) to repeat step b and c till obtained values are reasonably same as those obtained from previous iteration. 2 or 3 iterations are enough for convergence in error bound of ±0.1%. Q_b^n and C_b^n at down-stream of the control volume then are obtained from

$$Q_b^n = Q_f^n - Q_p^n \quad (10)$$

$$C_b^n = \frac{C_f^n Q_f^n - C_p^n Q_p^n}{Q_b^n}. \quad (11)$$

Q_b^n, C_b^n and C_p^n are also used as Q_f^{n+1}, C_f^{n+1}, and initial value of C_p^{n+1} in calculation of next control volume, respectively. Finally, total permeate flow rate and concentration for a given membrane with effective area of A are then

$$\overline{Q_p} = \sum_{n=1}^{N} Q_p^n \text{ (where } n = A/dA) \quad (12)$$

$$\overline{C_p} = \sum_{n=1}^{N} (Q_p^n \cdot C_p^n) \Big/ \overline{Q_p}. \quad (13)$$

3.3 Model Calibration Using System Operation Data

Field test on the pilot has been carried out from June to December 2001 at the experimental station on Coconut Island, Hawaii. In this period, atmospheric wind speed was 2 – 8 m/s. Artificial sodium chloride solution was used as feed water and its concentration was adjusted at around 4,000 ppm. Temperature of the feed was kept within 22 – 25°C during the test. Flow rate was measured at discharge port of the pump, outlet of the stabilizer, and concentrate port of the RO module. Pressure in the stabilizer was also measured and concentrations of the feed, product, and concentrate were measured at every 15 minutes with conductivity-meter. Wind speed and blowing direction were monitored with cup-type wind-speedometer and wind direction vane installed in vicinity of the windmill. All of the measured values were scanned at every 2 seconds and their averages over 30 seconds were recorded at every half minute. The experiment was focused on evaluation of pumping performance as a function of wind speed and RO performance variation with respect to feed conditions. 5 runs of the experiments for overall system performance were conducted and additional 4 runs of experiments for wind-energy conversion were carried out.

Figure 4 shows experimental results of August 24, 2001. The time-wise variations of wind speed, feed flow rate, pressure in the stabilizer, recovery ratio, and salt rejection are displayed in this figure. Although most of parameters are

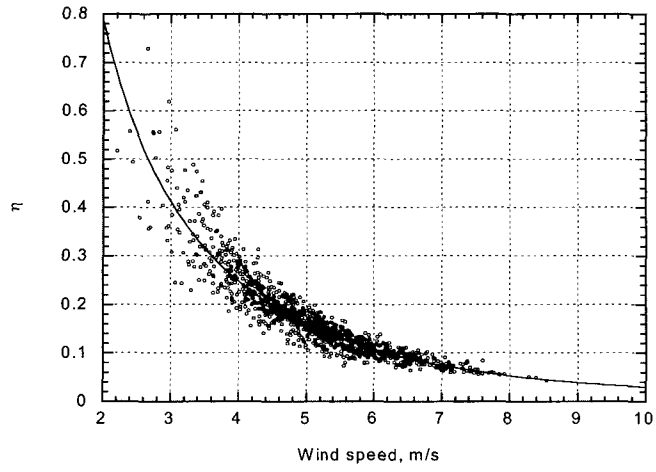

Fig. 5 Overall power coefficient of windmill/pump module with respect to wind speed

Table 1. Summary of the result of the system performance test

6/19	3.72, 8.32*	4050	0.511, 2.25	0.077, 0.34	594, 86.1	15.1	90.7
7/3	3.80, 8.50*	4010	0.604, 2.66	0.086, 0.38	592, 85.8	14.3	91.0
7/6	4.15, 9.28*	3980	0.631, 2.78	0.095, 0.42	603, 87.5	15.1	92.3
8/24	4.57, 10.2	4020	0.643, 2.83	0.093, 0.41	609, 88.3	14.5	91.6
12/4	5.91, 13.2	3990	0.790, 3.48	0.104, 0.46	612, 88.8	13.2	93.0

*: Estimated value by windmill/pump performance analysis

strongly dependent on wind speed, relatively stable performance was achieved without any trouble or failure during the monitored period as shown in the figure. Table 1 is a summary of field test results for system performance.

The overall efficiency of the windmill/pump module was calculated from Eq. (3) and plotted in Fig. 5. In this figure, discrete dots are obtained from experimental data and solid line is a regression curve. As shown in the figure, all dots are correlated well with the curve. This curve can be expressed in an equation.

$$\eta \approx 0.73\exp(-0.438U) + 1.89U^{-1.99} \qquad (14)$$

The overall efficiency is exponentially decreased as wind speed increases as shown in the figure, which was caused by a regulating device of the windmill. In many cases, it is desirable that the rotational speed of windmill keeps a constant value whatever the wind speed variations may be. Thus, in most conventional multi-blade windmills, a kind of rotational speed regulator is used and these systems are also used for power limitation and to reduce the forces acting on the blades when the wind speed is very high for structural safety [Le Gourieres, 1982]. An articulated tail vane is used as the regulator in the present windmill and the effective swept area decreases as the wind speed in-

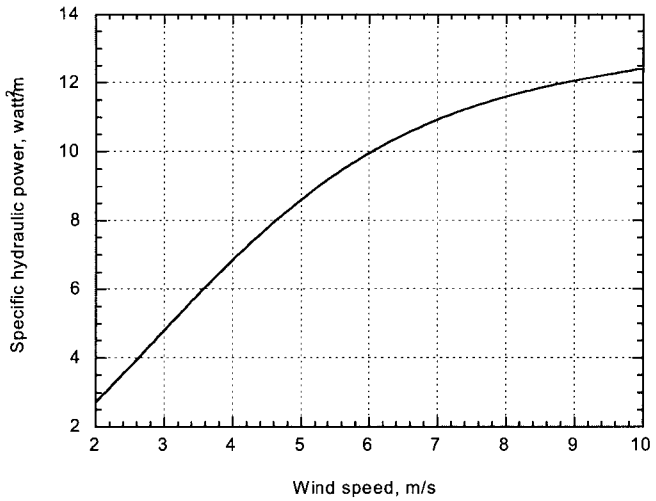

Fig. 6 Feasible specific hydraulic power of a windmill/pump module

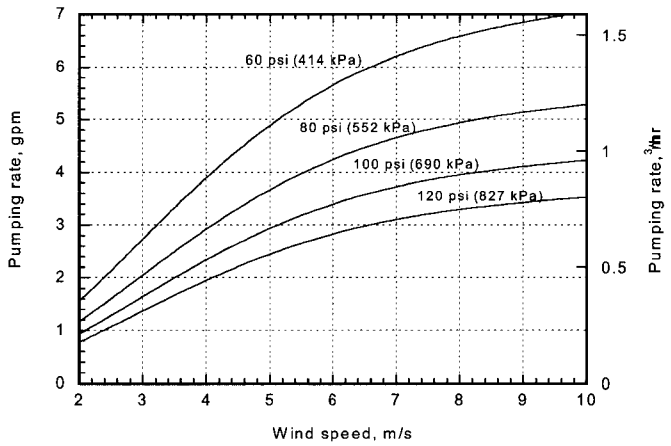

Fig. 7 Expectable pumping rate for various operating pressure with respect to `wind speed in case of 4.28 m (14 foot) windmill

creases. Eventually, this brings about a decline of the windmill efficiency. On the other hand, relatively higher values of η in case of mild wind condition may be owing to rotational inertia of the windmill.

From Eq. (14), feasible specific hydraulic power (hydraulic power per unit swept area) was obtained then as a function of wind speed for general application. Figure 6 shows the calculation result. Using this relationship and Eq. (2), expectable performance of a multi-blade windmill – piston pump module at a given con-dition can be calculated roughly. An example for 14-foot (4.28 m) windmill is shown in Fig. 7.

Now, we can predict membrane performance if inlet condition and permeability coefficients are given. Generally, a membrane element has its own permeability coefficients, k_w and k_i be-

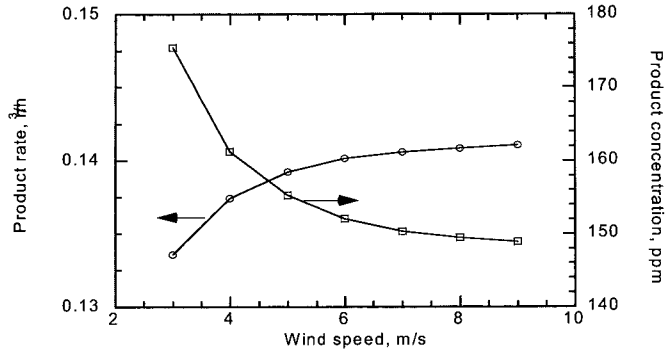

(a) Fixed operating pressure, p = 621 kPa (90 psi) and feed concentration, C_f = 2500 ppm

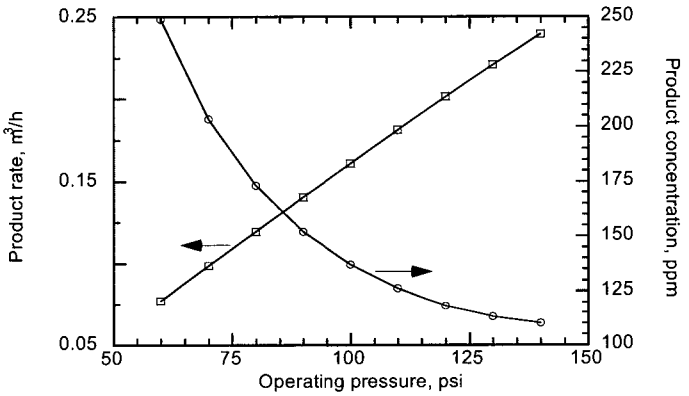

(b) Fixed wind speed, U = 6 m/s and feed concentration, C_f = 2500 ppm

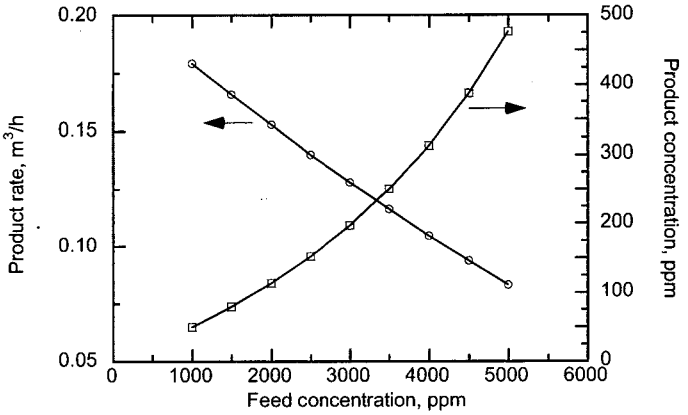

(c) Fixed wind speed, U = 6 m/s and operating pressure, p = 621 kPa (90 psi)

Fig. 8 Performance behavior of the present system by the prediction method of this work

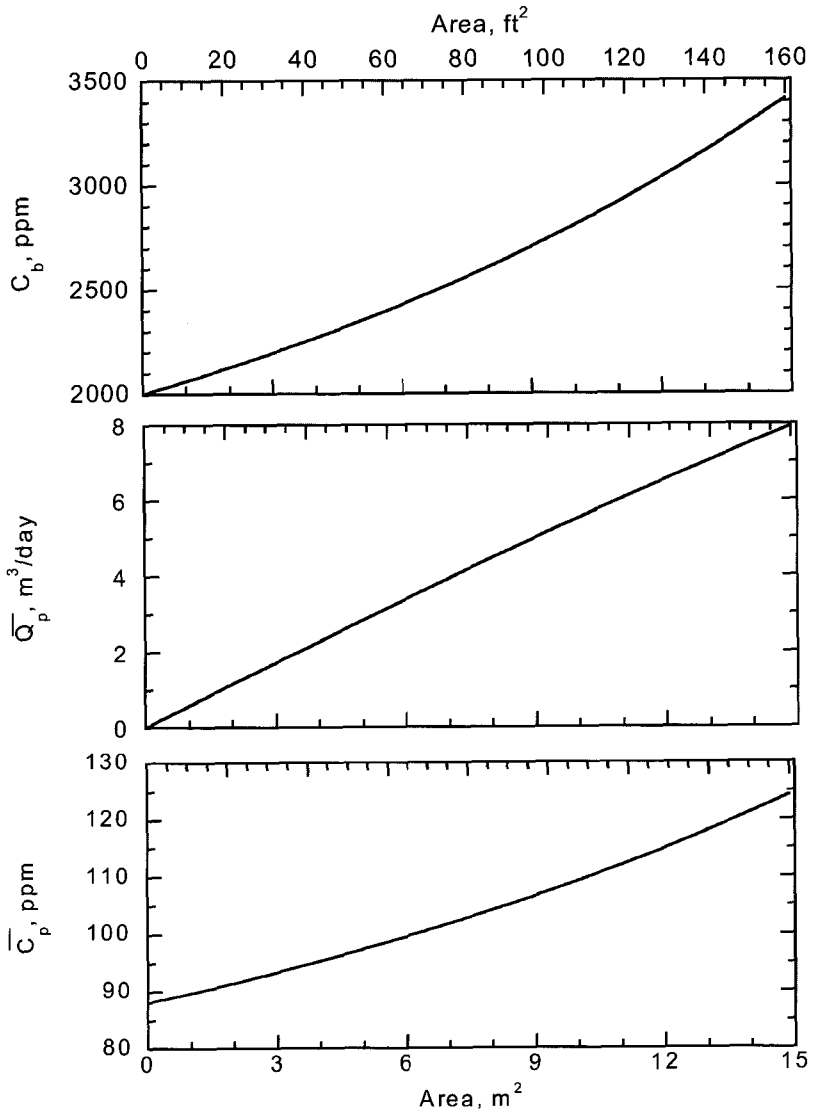

Fig. 9 Variations of concentration of brine, product rate, and concentration of product with respect to effective membrane area in case of $U = 6$ m/s, $C_f = 2{,}000$ ppm, and $p = 690$ kPa (100 psi)

cause they are characteristic physical properties determined by its material and structure which means that there are no universal coefficients that can be applied to any membrane. However, membranes in a same grade have coefficient values in a narrow range. The coefficients of the membrane element used in this work were obtained from standard performance data given by table 2, which are averages of the experimental result listed in table 1. From Eq. (4) and (5),

$$k_w = \frac{Q_p}{A\{p - 0.0779(C_r - C_p)\}} \quad (15)$$

$$k_i = \frac{C_p Q_p}{A(C_r - C_p)} \quad (16)$$

where C_r is representing concentration of the brine flow in an entire membrane module. Assuming

$$C_r = (C_f + C_b)/2, \quad (17)$$

k_w is 4.47×10^{-5} m/hr·kPa (1.26×10^{-4} gpm/ft^2·psi) and k_i is 1.12×10^{-3} m/hr (4.57×10^{-4} gpm/ft^2) through some manipulations. In order to verify the assumption of Eq. (17), a comparison was done between two values obtained by differential method and by using Eq. (5), (7), and (17). The deviation is only 0.3% because concentration profile of brine flow is nearly linear along the element. It means that the assumption of Eq. (17) is effective.

3.4 Performance Prediction

By combining results of above two sections, performance of a wind powered RO system under a given condition can be predicted. First, the feed flow rate is calculated from Eq. (14) at given windmill size, wind speed, and operating pressure. And then performance variables for a given membrane area are obtained from Eq. (12) & (13). This procedure can be easily done with a spreadsheet software. Figure 8 shows performance trend of a system that have the same configuration as the present prototype system. As shown in this figure, the effect of operating pressure on RO performance is much greater than that of wind speed. It implies that it is better to make operating pressure as high as possible, only that other design parameters infringe the constraints.

Variations of brine concentration, product rate, and product concentration as a function of effective membrane area were plotted in Fig. 9. Here, product rate and concentration at $A = A'$ are accumulated values from $A = 0$ to $A = A'$ from Eq. (12) & (13).

4. SYSTEM OPTIMIZATION AND THE DEVELOPMENT OF A DESIGN GUIDE

As shown in Fig. 9, product rate increases in nearly linear proportion to the membrane area but product quality gets worse in greater area due to increase of the brine concentration along the flow direction. Therefore, there exists limit of the membrane area for each feed condition. In addition, some operating limits (or constraints) have to be considered in design and selection of a system. That is to say, product quality and membrane lifetime should be considered as well as product quantity. In general, membrane manufacturers provide application and operational specifications (or limits) that are very similar to those of others in the same membrane grade. Considering the data for ultra-low- pressure RO membrane and the regulation for potable water, optimal system design problem may

Table 2. Reference RO performance of present prototype system

Parameter	Reference value
Membrane Area	7.43 m^2 (80 ft^2)
Pressure	621 kPa (90 psi)
Feed concentration	4,000 ppm (TDS)
Feed flow rate	0.738 m^3/hr (3.25 gpm)
Product rate	0.103 m^3/hr (0.455 gpm)
Salt rejection ratio	92.0 %
Recovery ratio	14.0 %

Table 3. Classification of the RO membrane arrangement.

Case	Arrangement	Effective area	Maximum recovery ratio
A	2540 × 1	2.32 m^2 (25 ft^2)	15 %
B	2540 × 2	4.65 m^2 (50 ft^2)	25 %
C	2540 × 3	6.97 m^2 (75 ft^2)	35 %
D	4040 × 1	7.43 m^2 (80 ft^2)	15 %
E	4040 × 1 + 2540 × 1	9.75 m^2 (105 ft^2)	20 %
F	4040 × 2	14.9 m^2 (160 ft^2)	25 %

be defined as follows.

Objective function: maximize product rate $Q_p = f(p, C_f, U,$ and membrane arrangement)

Constraints:

$60 \le p \le 140$ psi ($414 \le p \le 965$ kPa) (i)

$Q_b/Q_p \ge 5$ (at any element) (ii)

$C_p \le 400$ ppm (iii)

$Q_f \le 6$ gpm (1.4 m^3/hr) for 2540, 16 gpm (3.6 m^3/hr) for 4040 (iv)

maximum recovery: 15, 25, 35 % for 1, 2, and 3 stages, respectively (v)

This is a typical constrained multi-variable optimization problem that can be easily solved with several simple methods of optimization [Siddall, 1982]. The objective function may be modified according to user's demand. Minimum capital cost or minimum recovery period can be considered as an objective function. A combination of these considerations can be applicable to this problem as well. The first constraint arises from practically available pressure range achieved with a conventional windmill/pump module and a pressure stabilizer. Constraints (ii), (iv), and (v) are relevant to the lifetime and the stability of a membrane module. Violation of these constraints may bring about excessive concentration polarization, which can result in serious membrane fouling. And constraint (iii) is confined from drinking water recommendation

Table 4. Optimal membrane arrangement and operating pressure of a 4.3 m (14ft) windmill/RO system from viewpoint of maximum product rate

14-foot Windmill		Feed Water Concentration (TDS, ppm)									
		1000		2000		3000		4000		5000	
Averaged Wind Speed (m/s)	3	C	552	C	621	C	621	C	690		
		0.15	61	0.14	129	0.11	222	0.11	315		
	4	F	414	F	414	F	483	C	827	C	896
		0.22	80	0.17	195	0.16	308	0.15	245	0.14	324
	5	F	414	F	483	F	552	C	896	C	965
		0.22	77	0.21	162	0.20	258	0.17	215	0.16	283
	6	F	483	F	483	F	552	F	621	C	965
		0.27	67	0.22	158	0.21	250	0.20	351	0.16	269
	7	F	483	F	552	F	552	F	621	C	965
		0.27	66	0.26	138	0.21	246	0.20	344	0.17	261
	8	F	483	F	552	F	621	F	621	C	965
		0.27	65	0.26	137	0.25	216	0.20	340	0.17	257

1: Membrane configuration type shown in table 3.

2: Operating pressure (kPa) : 414=60psi, 483=70psi, 552=80psi, 621=90psi, 690=100psi, 758=110psi, 827=120psi, 896=130psi, and 965=140psi.

3: Product rate (m^3/hr)

4: Product salinity (ppm)

Table 5. An example of concept design for a wind-driven RO desalination system

• Averaged wind speed: 6 m/s • Feed concentration: 2,500 ppm • Desired product rate: more than 4 m^3/day (0.73 gpm)

Windmill diameter	Membrane arrangement	Pressure (psi / kPa)	Product rate (gpm / m^3/h)	Product salinity	Recovery ratio
12 feet (3.7 m)	C (2540×3)	110 / 758	0.74 / 0.17	134 ppm	32 %
	F (4040×2)	70 / 483	0.82 / 0.19	230 ppm	23 %
14 feet (4.3 m)	C (2540×3)	120 / 827	0.83 / 0.19	116 ppm	30 %
	F (4040×2)	80 / 552	1.01 / 0.23	191 ppm	24 %

brane configurations for small wind powered RO systems. For convenience, parallel arrangements were not considered here and spiral wound type 2540 and 4040 elements for brackish water were selected as an available membrane element. Table 4 shows the result of optimal concept design obtained with the above-mentioned procedure in case of 14-foot (4.28 m) windmill. Optimal membrane arrangement/operating pressure and expectable product rate/salinity are presented for each set of wind speed and feed concentration in this table. In most cases, two or more serial arrangement of membrane element has an advantage over one element module with same effective area from the viewpoint of maximization of the output. It is due to its lower required minimum brine flow. As found in the table, the optimal operating pressure is proportional to the feed concentration. Naturally, optimal design for other windmill size can be also accomplished by changing input value of windmill diameter.

Table 5 is an example of a concept design. Design condition is listed in upper half of the table. Finally, 4 possible system layouts of membrane arrangement and operating pressure were obtained through the above mentioned prediction method. The first one cost relatively less than others but its performance margin is very tight. The last one shows contrary trend. Considering installation cost and details, designer can select one among them, which is most appropriate for his/her own situation. In addition to this, more careful review is required when wind speed at a site varies in relatively wider range.

To improve the availability of this work, it is pending as a further study to consider concentration polarization on the membrane surface because the present RO design tool may carry relatively significant error in case of low feed rate and rich raw water.

5. CONCLUSIONS

An experiment on system performance was conducted in order to study energy balance and system behavior of a wind powered reverse osmosis desalination pilot. The prototype system developed at university of Hawaii performed stably and effectively. At average wind speed of 5 m/s, product rate is about 2.3 m^3/day (600 GPD) and salt rejection ratio is about 92% for the feed water salinity of 4,000 ppm (TDS). Any trouble and failure were not found during the field test, even in mild wind condition. It is mainly due to adoption of a pressure stabilizer and brine flow control method.

Based on the membrane process simulation, a basic and simple design tool has been suggested for wind powered RO desalination. This tool can predict system performance at given wind speed and feed concentration. And then a concept design criterion was presented for 14-foot (4.28 m) windmill and low pressure RO system by using windmill/pump performance curve and permeability coefficients obtained from the experimental results. In general, performance curve and permeability coefficients vary according to model and system configuration but they have same order of magnitude. Thus, it can be applied to the first step of concept design of a similar type wind powered RO system. Furthermore, if the performance curve and permeability coefficients are given for a particular case, more realistic predictions could be made by the method described above.

ACKNOWLEDGEMENTS

The authors gratefully acknowledged the financial support of the Korea Science & Engi-

neering Foundation (KOSEF) to the senior author.

REFERENCES

Abdul-Fattah, A.F. (1986). "Selection of solar desalination system for supply of water in remote arid zone," *Desalination*, Vol.60, pp.165-189.

AWWARF (American Water Works Association Research Foundation), LdE (Lyonnaise des Eaux), and WRC (Water Research Commission) (1996). *Water Treatment Membrane Process*, McGraw-Hill, New York.

Denisov, G.A. (1994). "Theory of Concentration Polarization in Cross-Flow Ultrafiltration: Gel-Layer Model and Osmotic Pressure Model," *Journal of Membrane Science*, Vol.91, pp.173-187.

Feron, P. (1985). "The use of wind-power in autonomous reverse osmosis seawater desalination," *Wind Engineering*, Vol.9, pp. 180-199.

Garcia-Rodriguez, L, Romero-Ternero, V., and Gomez-Camacho, C. (2001). "Economic analysis of wind-powered desalination," *Desalination*, Vol.137, pp.259-265.

Hicks, D., Pleass, C., Mitcheson, G.R., and Salevan, J. (1989). "Delbouy: Ocean wave-powered seawater reverse osmosis desalination systems," *Desalination*, Vol.73, pp.81-94.

Houcine, I., Benjemaa, F., Chahbani, M., and Maalej, M. (1999). "Renewable energy source for water desalting in Tunisia," *Desalination*, Vol.125, pp.123-132.

Kellogg, W.D., Nehrir, M.H., Venkataramanan, G., and Gerez, V. (1998). "General unit sizing and cost analysis for stand-alone wind, photovoltaic, and hybrid wind/PV systems," *IEEE Transaction on Energy Conversion*, Vol.13(1), pp.70-75.

Kiranoudis, C.T., Voros, N.G., and Maroulis, Z.B. (1997). "Wind energy exploitation for reverse osmosis desalination plants," *Desalination*, Vol.109, pp.195-209.

Le Gourieres, D. (1982). *Wind Power Plant: Theory and Design*, Pergamon Press, Oxford.

Liu, C.C.K., Park, J., Migita, R., and Qin, G. (2002) "Experiments of a prototype wind-driven reverse osmosis desalination for remote Pacific islands," *Desalination,, in Review.*

Lonsdale, H.K., Merten, U., and Riley, R.L. (1965). "Transport Properties of CA Osmotic Membranes," *Journal Applied Polymer Science*, Vol.9, pp.1341-1362.

Merten, U., Lonsdale, H.K., and Riley, R.L. (1964). "Boundary-Layer Effects in Reverse Osmosis," *Industrial Engineering Chemistry Fundamentals*, Vol.3(3), pp.210-213.

Parekh, B.S. (1988). *Reverse Osmosis Technology – Application for High-Purity-Water Production*, Marcel Dekker, Inc., New York.

Reynolds, T.D. and Richards, P.A. (1996). *Unit Operations and Processing in Environmental Engineering*, Houghton Mifflin, Boston, MA, USA.

Robinson, R., Ho, G., and Mathew, K. (1992). "Development of a reliable low-cost reverse osmosis desalination unit for remote communities," *Desalination*, Vol.86, pp.9-26.

Rosenfeld, J., Loeb, S. (1967). "Turbulent region performance of reverse osmosis desalination tubes," *I & EC Process Design and Development*, Vol.6(1), pp.123-127.

Siddall, J.N. (1982). *Optimal Engineering De-*

sign, Marcel Dekker, Inc., New York and Basel.

Voivontas, D., Misirlis, K., Manoli, E., Arampatizis, G., and Assimacopoulos, D. (2001). "A tool for the design of desalination plants powered by renewable energies," *Desalination*, Vol.133, pp.1175-198.

Wangnick, K. (1996). *1996 IDA worldwide desalting plants inventory report no. 14*, IDA (International Desalination Association), Topsfield, MA, USA.

Weiner, D., Fisher, D., Moses, E.J., Katz, B., and Meron, G. (2001). "Operation experience of a solar- and wind-powered desalination demonstration plant," *Desalination*, Vol.137, pp.7-13.

White, F.M. (1986). *Fluid Mechanics, 2nd Ed.*, McGraw-Hill, New York, Ch.11.

WHO (World Health Organization) (1971). *International Standards for Drinking Water*, 3rd Ed., Geneva.

NOMENCLATURE

A	Area (m^2)
C	Concentration (ppm, TDS: total dis solved solid)
g	Acceleration of gravity (m/s^2)
H	Total head (m)
J	flux (m/hr)
k	Permeability coefficient
$\dot{m}$	Mass flow rate (kg/s)
P	Power (watt)
p	Pressure (kPa)
Q	Flow rate (m^3/s)
T	Temperature (°C)
t	Time
U	Wind speed (m/s)
Overall	efficiency
π	Osmotic pressure (kPa)
ρ	Density (kg/m^3)

Subscript

a	Air
avail	Available
b	Brine
deliv	Delivered
f	Feed
i	Salt
p	Product
w	Water

Thermo-Fluid System Dept., Korea Institute of Machinery & Materials, Daejeon, Korea (E-mail : giant@kimm.re.kr)

Dept. of Civil Engineering, University of Hawaii at Manoa, Honolulu, Hawaii, USA